Genome-wide Identification and Stress-Responsive Expression Analysis of the ARR-B Gene Family in Watermelon (Citrullus lanatus)

Huan Li
Henan Agricultural University
Aofeng Hu
Henan Agricultural University
Yaxin Chen
Henan Agricultural University
Wenlu Kang
Henan Agricultural University
Junling Dou
Henan Agricultural University
Huanhuan Niu
Henan Agricultural University
Wenkai Yan
Henan Agricultural University
Junyi Tan
Henan Agricultural University
Huayu Zhu
Henan Agricultural University
Luming Yang
Henan Agricultural University
Dongming Liu
liudongming5668@163.com

Henan Agricultural University

Research Article

Keywords: ARR-B transcription factor, Watermelon, Bioinformatics analysis, Tissue expression patterns, Abiotic stress

Posted Date: June 26th, 2026

DOI: https://doi.org/10.21203/rs.3.rs-9980420/v1

Additional Declarations: No competing interests reported.

Abstract

Background Type-B response regulator (ARR-B) genes act as positive regulators of cytokinin signal transduction and exert essential functions in plant growth, development, and abiotic stress tolerance. Nevertheless, systematic genome-wide identification and functional characterization of the ARR-B gene family have not been comprehensively performed in watermelon, an economically important crop vulnerable to diverse abiotic stresses.

Results In this study, a total of 10 ARR-B family genes were identified from the watermelon reference genome, and their physicochemical properties, gene structures, conserved cis-elements, tissue expression patterns and abiotic stress response characteristics were systematically analyzed using bioinformatics approaches. Subcellular localization prediction showed that nine ClARR-B proteins were localized in the nucleus, while only *ClARR-B4* was distributed in the cytoplasm. Chromosome mapping revealed that ClARR-B genes were unevenly distributed on watermelon chromosomes, with five members located on chromosome 6, accounting for the largest number of family members. Multiple cis-acting elements related to growth and development, hormone response, biotic and abiotic stresses were identified in the promoter regions of ClARR-B genes. The qRT-PCR results indicated that *ClARR-B1* and *ClARR-B2* were highly expressed in watermelon roots, stems, leaves, flowers and fruits, suggesting their critical roles in the growth and development of major watermelon organs. Compared with the control, *ClARR-B4*, *ClARR-B7* and *ClARR-B9* were markedly upregulated under drought stress, while *ClARR-B2* and *ClARR-B6* displayed the strongest upregulation under salt stress. *ClARR-B4* was the most significantly induced by cold stress. Collectively, *ClARR-B4* is involved in the responses of watermelon to drought and cold stresses, laying a solid basis for subsequent studies on abiotic stress tolerance.

Conclusion A total of ten ARR-B transcription factor family members were identified in watermelon, which are extensively involved in watermelon growth, development and abiotic stress response. This study provides a theoretical basis for further exploring the molecular functions of the ARR-B gene family in watermelon development and stress resistance.

Introduction

As an annual trailing herbaceous crop in the Cucurbitaceae family, watermelon (*Citrullus lanatus*) is rich in vitamins, citrulline and lycopene. It is widely consumed worldwide as fresh fruit and processed products, including juice, confectionery and sauces. However, watermelon is frequently exposed to various adverse conditions, including salt, drought, cold, heat, and pathogen stresses, which severely restrict its yield and quality [1, 2]. Transcription factors serve as core molecular switches governing gene expression, thereby playing essential roles in plant abiotic stress adaptation [3]. Multiple transcription factor families, including C2H2-ZFP, HD-ZIP, WRKY, and B-Box Zinc Finger, have been functionally characterized in watermelon. These regulatory proteins positively modulate plant stress acclimation, thereby orchestrating vegetative growth, developmental progression, and yield stability under unfavorable environmental conditions [4–7]. Authentic Response Regulator (ARR) genes are key

components of the histidine-aspartate (His-Asp) phosphorylation signal transduction pathway prevalent in prokaryotes and plants [8–10]. This phosphorelay system is particularly essential in plants, which transmits signals from the cell periphery to the nucleus to regulate a variety of growth and developmental processes [11–13]. ARRs in plants are mainly divided into three categories: type-A, type-B and pseudo-type, each with unique structural characteristics and functional patterns[11, 14]. In Arabidopsis thaliana, the transcription of type-A ARR genes can be rapidly induced by cytokinins. They mainly act as negative regulators in cytokinin signal transduction and fine-tune signal intensity by forming negative feedback loops [14–15].Type-B ARRs serve as positive regulators in plant cytokinin signal transduction and play vital roles in plant growth and development [16]. Type-B ARRs contain two conserved domains: a receiver domain involved in phosphorylation, and a large C-terminal extension that harbors a GARP (G2-like, ARR, Psr1) motif with Myb-like DNA-binding properties. The receiver domain undergoes phosphorylation modification and harbors a conserved REC domain that governs the transcriptional activation of cytokinin-responsive genes [17]. Although the C-terminal sequences of type-B ARR members exhibit substantial structural variability, all isoforms retain a conserved 60-amino-acid segment that shares high sequence homology with the mammalian Myb repeat domain, which is essential for the sequence-specific DNA binding and transcriptional activation of target genes involved in the cytokinin response [18–20]. In Arabidopsis thaliana, type-B ARRs are divided into three subfamilies based on phylogenetic analysis. Subfamily 1 comprises seven members, while Subfamilies 2 and 3 each contain two members. These subfamily members exert distinct yet complementary functions in cytokinin responses, with members of Subfamily 1 playing a predominant role [21]. Pseudo-type ARRs, such as ARR15 to ARR17, lack the canonical N-terminal receiver domain, which indicates that they may not participate directly in the phosphorelay pathway, yet could still regulate cytokinin signaling via alternative mechanisms [22].

Plant hormones participate in the entire life cycle of watermelon and play vital roles. As positive regulators of cytokinin signal transduction, ARR-Bs are involved in nearly all aspects of plant growth and development, including cell division, light responses and bud initiation. Beyond cytokinin signal transduction, ARR-Bs are also associated with sodium accumulation, root elongation, callus formation, as well as tolerance to phosphate stress and cold stress. Meanwhile, endogenous cytokinin levels are closely linked to pleiotropic developmental changes [23–25]. To date, the ARR-B gene family has been reported in numerous species, including rice [26], tomato [27], peach [28], and soybean [29]. However, comprehensive research on the ARR-B transcription factor family in watermelon remains limited, and its biological functions have not yet been elucidated.

In this study, we performed genome-wide bioinformatics analysis to identify the number of ARR-B genes associated with growth and development in watermelon. We further characterized their physicochemical properties, subcellular localization, phylogenetic relationships, chromosomal distribution, gene structures and cis-acting elements in promoter regions. Additionally, the watermelon line G42 with stable genetic traits was used to investigate tissue and stress-responsive expression patterns. This work aims to provide a reference for further exploring the evolutionary characteristics and biological functions of ARR-B genes.

Results

Identification of the ARR-B genes in watermelon

ARR-B proteins contain two conserved domains (PF00072 and PF00249). In watermelon, 39 genes harbor PF00072 and 260 genes possess PF00249, while only 10 members carry both conserved domains simultaneously. These genes were designated *ClARR-B1* to *ClARR-B10* sequentially according to their gene IDs (Table 1).

Physicochemical property analysis revealed that number of amino acids ranged from 331 (*ClARR-B4*) to 698 (*ClARR-B10*), and the protein isoelectric points varied from 5.30 (*ClARR-B10*) to 7.24 (*ClARR-B9*). Subcellular localization prediction indicated that only *ClARR-B4* was localized in the cytoplasm, whereas all the other members were targeted to the nucleus (Table 1), which is consistent with the characteristics of ARR-B genes as transcription factors.

Table 1
Prediction of physicochemical properties and subcellular localization of ClARR-B gene family members

Gene names	Gene ID	Chromosome	Amino acid length	Isoelectric point	Subcellular localization
ClARR-B1	Cla97C05G087920.1	Chr05	661	5.83	cell nucleus
ClARR-B2	Cla97C06G114280.1	Chr06	664	5.81	cell nucleus
ClARR-B3	Cla97C06G121390.1	Chr06	687	6.20	cell nucleus
ClARR-B4	Cla97C06G122690.1	Chr06	331	6.09	cytoplasm
ClARR-B5	Cla97C05G097440.1	Chr05	689	5.97	cell nucleus
ClARR-B6	Cla97C08G161150.1	Chr08	584	5.42	cell nucleus
ClARR-B7	Cla97C06G122670.1	Chr06	439	6.24	cell nucleus
ClARR-B8	Cla97C01G006220.1	Chr01	609	6.02	cell nucleus
ClARR-B9	Cla97C06G109970.1	Chr06	554	7.24	cell nucleus
ClARR-B10	Cla97C11G210080.1	Chr11	698	5.30	cell nucleus

Chromosomal location and gene structure of the ClARR-B Gene Family

Chromosomal localization analysis showed that the ten members of the watermelon ClARR-B gene family were unevenly distributed across five distinct chromosomes (Fig. 1). Chromosome 6 harbored the largest number of members (five), while Chromosome 5 contained two members. Chromosomes 1, 8 and 11 each carried one ClARR-B gene, and no homologs were detected on the remaining chromosomes. *ClARR-B4* and *ClARR-B7* were closely adjacent on Chromosome 6, suggesting that they form a tandem duplication gene cluster.

As shown in Fig. 2, all ClARR-B genes contained introns with a relatively narrow range in number, varying from 4 to 6. *ClARR-B6* and *ClARR-B8* had four introns. *ClARR-B1*, *ClARR-B2*, *ClARR-B3*, *ClARR-B5* and *ClARR-B7* shared the same intron count of five. *ClARR-B4*, *ClARR-B9* and *ClARR-B10* possessed six introns.

Green bars represent the five chromosomes with ClARR-B genes. The scale indicates the chromosome length, and the blue lines indicate the position of each ClARR-B gene.

Exon-intron structure of ClARR-B genes. Yellow boxes and black lines represent exons and introns. The scale indicates the gene length

Phylogenetic Analysis of the ClARR-B Gene Family

We retrieved ARR-B sequences from the databases of muskmelon, cucumber, wax gourd, bottle gourd, Arabidopsis thaliana and wheat, and verified them via conserved domain analysis. A total of 7, 7, 7, 7, 14 and 25 ARR-B genes were identified from the above species, respectively. The amino acid sequences encoded by these genes and the 10 ClARR-B genes were aligned using MUSCLE and Jalview, and a phylogenetic tree was constructed with IQ-TREE.

As shown in Fig. 3, all ARR-B genes were clustered into three major clades: Class Ⅰ, Class Ⅱ and Class Ⅲ. Class Ⅲ was further divided into two subgroups, IIIA and IIIB. Among the 10 ClARR-B genes, one belonged to Class Ⅱ and another to Class Ⅰ. In Class Ⅰ, *ClARR-B8* shared the closest phylogenetic relationship with *AT1G68210.1*. In Class Ⅱ, *ClARR-B9* was closely related to three Arabidopsis genes, namely *AT2G27070.1*, *AT4G00760.1* and *AT5G07210.1*.

Five ClARR-B genes were assigned to Class IIIA. *ClARR-B1* and *ClARR-B2* showed the highest homology with *AT3G16857.2* and *AT4G16110.1*; *ClARR-B6* was most closely related to *AT1G67710.1*; *ClARR-B4* and *ClARR-B7* also fell into Class IIIA. The remaining three ClARR-B members belonged to Class IIIB. *ClARR-B5* had a close genetic relationship with *AT2G25180.1* and *AT4G31920.1*, while *ClARR-B3* and *ClARR-B10* were grouped together within Class IIIB.

The phylogenetic tree is divided into four groups (Class Ⅰ, Class Ⅱ, Class ⅢA and Class ⅢB)

The background is shaded in purple, yellow, green,and blue for Class Ⅰ, Class Ⅱ, Class ⅢA and Class ⅢB, respectively

Analysis of conserved motifs of the ClARR-B gene family

The results of conserved motif analysis for the ClARR-B gene family are presented in Fig. 4. A total of ten highly conserved motifs were identified, designated Motif 1 to Motif 10. Among them, Motif 1 corresponds to the *PEC-typeB-ARR-like* motifs and exists in all family members.

Motif 1, Motif 2, Motif 3, Motif 4 and Motif 5 were detected in all ten ClARR-B genes. This indicates that the motifs of the ClARR-B gene family are highly conserved. In addition, ClARR-B genes within the same subfamily with close phylogenetic relationships share highly conserved structural compositions and motif distributions.

Distribution of conserved motifs in ClARR-B proteins. Different motifs are represented by numbered colored boxes. The scale indicates the gene length

Analysis of cis-acting elements in the promoters of ClARR-B genes

Cis-acting elements play vital roles in the regulation of gene expression. Genes with analogous functions usually possess similar regulatory elements in their promoter regions. To further explore the expression and regulatory mechanisms of ClARR-B family genes, we extracted the 2000 bp genomic sequences upstream of each ClARR-B member and predicted their cis-acting elements using the PlantCARE database.

As shown in Fig. 5, a total of 32 distinct cis-acting elements were identified. Four major categories were detected in nearly all ClARR-B promoters: core promoter elements, elements associated with abiotic stress responses, hormone responses, and plant growth and development.

Stress-related elements included light-responsive elements, anaerobic induction elements, defense and stress-responsive elements, low-temperature-responsive elements and wound-responsive elements. Most ClARR-B promoters harbored hormone-related cis-elements, such as those responding to methyl jasmonate (MeJA), gibberellin, salicylic acid, abscisic acid and auxin. Additionally, multiple elements linked to growth and development were found, including motifs related to seed storage protein metabolism, meristem-specific expression and endosperm expression.

Collectively, the ClARR-B gene family in watermelon is likely involved in the regulation of diverse abiotic stress responses, hormone signaling, as well as plant growth and development.

Distribution of conserved promoter cis-elements in ClARR-B promoters. Different motifs are represented by numbered colored boxes. The scale indicates the promoter length

Secondary and Tertiary Structures of ClARR-B Proteins

The secondary structures of watermelon ClARR-B proteins are mainly composed of α-helix, extended strand, β-turn and random coil. Random coils and α-helices constitute the major structural frameworks, while β-sheets account for the smallest proportion.

Homology modeling of tertiary structures revealed obvious differences in the proportion of structural components among members from different subfamilies. Within Class IIIA, *ClARR-B4* shared highly similar structures with *ClARR-B7*, and so did *ClARR-B1* and *ClARR-B2*. By contrast, *ClARR-B3*, *ClARR-B5* and *ClARR-B10* in Class IIIB exhibited substantial structural variations (Fig. 6).

ARR-B proteins clustered on the phylogenetic tree generally possess similar tertiary structures, indicating structural and functional conservation. In contrast, proteins with divergent tertiary structures within the same phylogenetic clade are undergoing evolutionary differentiation.

Significant structural differences were observed among ClARR-B proteins from distinct phylogenetic subgroups

Tissue Expression Analysis of the ClARR-B Gene Family

To characterize the expression patterns of ClARR-B genes in watermelon, we performed quantitative real-time PCR (qRT-PCR) to detect their transcript levels in five tissues of watermelon line G42, including roots, stems, leaves, flowers and fruits. As shown in Fig. 7, the ClARR-B genes exhibited distinct expression profiles across different tissues.

In roots, *ClARR-B2* and *ClARR-B6* were highly expressed, followed by *ClARR-B1*, *ClARR-B3*, *ClARR-B5* and *ClARR-B10*, while the remaining genes showed low expression. In stems, *ClARR-B2* had the highest expression level, with *ClARR-B1*, *ClARR-B5* and *ClARR-B6* showing moderate expression. In leaves, *ClARR-B1* was the most highly expressed, and *ClARR-B2*, *ClARR-B5* and *ClARR-B10* displayed comparable expression levels with no obvious difference. In flowers, *ClARR-B2* showed the maximum expression, followed by *ClARR-B1*, *ClARR-B3*, *ClARR-B5* and *ClARR-B10*; other genes were weakly expressed. In fruits, *ClARR-B1* had the highest transcript abundance, and *ClARR-B2* and *ClARR-B5* ranked second.

Overall, *ClARR-B1* and *ClARR-B2* shared similar expression patterns and maintained relatively high expression in all tested tissues. The relative expression levels of *ClARR-B4*, *ClARR-B7* and *ClARR-B9* were all lower than 1 across all tissues.

Expression levels of 10 ClARR-B genes in different tissues of watermelon cultivar G42. Relative expression levels were quantified by qRT-PCR with ClActin as the internal reference, and calculated using the $2^{-\triangle\triangle Ct}$ method. Lowercase letters denote statistically significant differences ($P < 0.05$) among different genes within the same tissue, as determined by one way ANOVA followed by Tukey's test. Data are shown as mean ± SD (n = 3, biological replicates).

Expression Patterns of the ClARR-B Gene Family under Drought, Salt and Cold Stresses

To further elucidate the underlying responsive molecular mechanism of the ClARR-B gene family under abiotic stresses, watermelon seedlings were treated with drought, salt, and cold stresses. Leaf samples exhibiting apparent stress phenotypes were harvested, and qRT-PCR was applied to quantify the expression levels of ClARR-B genes under distinct stress conditions. Fv/Fm is a vital physiological parameter and core indicator evaluating photosynthetic capacity, which reflects the maximum photochemical efficiency and potential maximal light conversion efficiency of photosystem II. For most healthy plants, the Fv/Fm value maintains a stable high range of approximately 0.78–0.85, whereas stress exposure triggers a decline in this value. Such reduction signifies inhibited PSII function and decreased light energy conversion efficiency; accordingly, Fv/Fm serves as a reliable physiological indicator for plant physiological health status. The chlorophyll fluorescence parameter Fv/Fm decreased significantly in watermelon leaves under drought, salt, and cold stresses (Fig. 8). Specifically, Fv/Fm dropped from roughly 0.79 to 0.65 under drought stress, from approximately 0.79 to 0.54 under salt stress, and from around 0.79 to 0.08 under cold stress. These results demonstrated that all three abiotic stresses exert adverse impacts on watermelon growth and development, and caused obvious damage to watermelon seedlings. On this basis, the expression profiles of ClARR-B family genes were further analyzed at the phenotypic stress stage (Fig. 9).

ClARR-B family genes exhibited distinct expression specificity under different stress conditions. Under drought stress, *ClARR-B8* was significantly downregulated compared with the control, whereas *ClARR-B1/2/3/4/5/6/7/9/10* were significantly upregulated, among which *ClARR-B4*, *ClARR-B7*, and *ClARR-B9* showed the most prominent upregulation. Under salt stress, *ClARR-B4*, *ClARR-B7*, and *ClARR-B9* displayed no significant expression changes, while *ClARR-B5* and *ClARR-B8* were markedly downregulated, and *ClARR-B1/2/3/6/10* were significantly upregulated, with *ClARR-B2* and *ClARR-B6* presenting the highest induction. Under low-temperature stress, the expression levels of *ClARR-B7/8/9/10* remained unchanged, *ClARR-B5* and *ClARR-B6* were significantly downregulated, and *ClARR-B1/2/3/4* were significantly upregulated, with *ClARR-B4* showing the most substantial upregulation.

All three abiotic stresses markedly decreased the Fv/Fm values of watermelon leaves, indicating that the photosynthetic function of seedlings was severely impaired

Expression patterns of 10 ClARR-B genes under drought, salt and cold stresses in watermelon. Relative expression levels were determined by qRT-PCR using ClActin as an internal reference and calculated via the $2^{-\triangle\triangle Ct}$ method. Lowercase letters indicate statistically significant differences ($P < 0.05$) for the same gene among different abiotic stresses, as determined by one way ANOVA followed by Tukey's test. Data are presented as mean ± SD (n = 3, biological replicates)

Discussion

The evolutionary trajectory of plant Type-B Authentic Response Regulators (ARR-B) exemplifies the profound impact of gene duplication and subsequent adaptive evolution on the functional diversification of signaling networks. Phylogenomic analyses confirm that ARR-B genes, which serve as positive regulators in cytokinin signal transduction, originate from a common ancestral gene present in early land plants [29, 30]. The substantial interspecific variation in ARR-B copy number is primarily driven by whole-genome duplication (WGD) events, segmental duplications, and tandem amplifications, which provide the raw genetic material for evolutionary innovation [30, 31]. Following these duplication events, duplicated ARR-B copies undergo functional differentiation through mechanisms such as subfunctionalization and neofunctionalization, allowing plants to adapt to diverse environmental stresses and developmental requirements [32, 33]. This process is not merely a result of neutral drift but is significantly shaped by adaptive evolution, where specific domains of the ARR-B proteins experience positive selection to optimize cytokinin responses in lineage-specific contexts [34–35].

The ancestral origin of the ARR-B gene family is deeply rooted in the evolution of land plants. Type-B ARRs are characterized by a conserved N-terminal receiver domain and a C-terminal GARP DNA-binding motif, structures that are essential for their role in the two-component cytokinin signaling pathway [36–37]. In the present study, only 10 ClARR-B genes containing both canonical conserved domains PF00072 and PF00249 were identified in watermelon, although 39 watermelon genes carry PF00072 and 260 genes possess PF00249 alone. Comparative genomic studies across diverse species, including Brassica napus, tomato (*Solanum lycopersicum*), tea plant (*Camellia sinensis*), cucumber, muskmelon, wax gourd, bottle gourd, Arabidopsis thaliana and wheat, reveal that while the core structural domains remain highly conserved indicative of strong purifying selection, the overall family size varies significantly [27, 28, 34]. For instance, Brassica napus possesses 35 type-B ARR genes, an expansion attributed to its polyploid nature and recent whole-genome duplication events [30]; tomato contains 12 SlARR-B genes; 14 in Arabidopsis and 25 in wheat [27]. Watermelon owns 10 ClARR-B genes, slightly more than these four cucurbit crops but far fewer than polyploid wheat. The identification of 69 GARP transcription factors in tea plant, including the ARR-B subfamily, further underscores the widespread presence and diversification of this ancestral lineage across angiosperms [35]. These findings support the hypothesis that a single ancestral ARR-B gene existed prior to the divergence of major plant lineages, serving as the foundation for subsequent radiations [37].

Gene duplication acts as the primary engine for generating copy number variation (CNV) in the ARR-B family. Whole-genome duplication (WGD) and segmental duplication are identified as the main forces driving the expansion of BnARRs in Brassica napus, where duplicated genes were retained and classified into seven distinct phylogenetic groups [30]. Similarly, in apple (Malus × domestica), WGD events have been shown to drive the evolution of gene families, providing duplicated copies that serve as material for variation and potential new functions [34]. Tandem duplication, often mediated by short repeated sequences through unequal sister-chromatid exchange, also contributes to the amplification of specific gene clusters, offering potential material for adaptive evolution under environmental stress [31]. Consistently, our chromosomal location analysis found that *ClARR-B4* and *ClARR-B7* form a tandem duplication cluster on watermelon Chromosome 6, directly proving tandem duplication contributes to

watermelon ARR-B family expansion. In seashore paspalum (*Paspalum vaginatum*), 2,542 tandem duplicated genes were identified, with many showing enrichment in stress-response pathways, illustrating how local duplication events can rapidly expand gene repertoires relevant to adaptation [38]. The frequency of these duplication events varies across lineages, leading to the observed interspecific differences in ARR-B family size [39–40]. Our phylogenetic tree clustered all tested ARR-Bs into Class Ⅰ, Class Ⅱ and Class Ⅲ (III A/IIIB), consistent with evolutionary grouping patterns in previously reported species, further confirming conserved evolutionary topology of this gene family. Genes from the same phylogenetic clade share highly conserved exon-intron compositions and protein motif arrangements in watermelon, while clade-specific motifs lead to possible functional divergence among ClARR-B paralogs.

Following duplication, the fate of ARR-B copies is determined by a combination of neutral processes and adaptive evolution. While many duplicates are lost due to nonfunctionalization, those that are retained often undergo functional differentiation [41–42]. Subfunctionalization involves the partitioning of ancestral functions, such as tissue-specific expression patterns or response to specific stimuli, between duplicate copies [33, 43]. For example, in Arabidopsis thaliana, the histological expression domains of duplicated genes show distinct patterns, indicating that differentiation in expression is a key mechanism for maintaining duplicate copies [43]. In watermelon, divergent spatial expression across root, stem, leaf, flower and fruit, as well as differential induction upon drought, salt and cold stresses among 10 ClARR-B members, strongly supports subfunctionalization after gene duplication: *ClARR-B1/2/3* were universally upregulated under three stresses, whereas other genes displayed stress-type-specific upregulation or repression. Neofunctionalization, where one copy acquires a novel function, is also evident. In the case of the PICKLE gene family, a neofunctionalized duplicate, PICKLE RELATED 2, exhibits antagonistic effects to the ancestral gene on the seed transcriptome and is under positive selection [33]. This suggests that adaptive evolution plays a crucial role in shaping the functional landscape of duplicated genes, allowing them to contribute to new biological processes. In addition, abundant hormone- and stress-related cis-elements (ABRE, LTR, MBS, MeJA-responsive motifs etc.) were enriched in ClARR-B promoter regions, which endow watermelon ARR-B duplicates with diversified regulatory responsiveness to phytohormones and adverse environments during adaptive evolution. High-impact literature elucidates that ARR-Bs do not function in isolation but operate within extensive transcriptional networks that facilitate hormone cross-regulation and physiological resilience [44–45]. Under salt stress conditions, ARR-B genes exhibit distinct upregulation patterns that are critical for maintaining ion homeostasis. Recent studies demonstrate that specific ARR-B members, such as *LpARR10* in perennial ryegrass, are significantly induced by saline environments and confer tolerance by directly trans-activating the expression of SOS1 and SOS3, which are essential for sodium exclusion [46]. This mechanism establishes a direct molecular link between cytokinin signaling and the regulation of ion transporters. Similarly, in tomato, *SlARR-B1* and *SlARR-B12* display differential root expression under salt stress, contributing to early stress signal perception [26]. In Brassica napus, WGD-driven ARR-B expansion leads to functional diversification and enhanced salt adaptability [28]. Consistent with these findings, our study revealed that watermelon ClARR-B family members exhibit divergent salt-responsive patterns. Specifically, *ClARR-B1/2/3/6/10* were significantly induced under salt stress, while *ClARR-B5/8*

were repressed, and *ClARR-B4/7/9* remained stable, indicating functional differentiation of ClARR-B paralogs in salt stress adaptation.

Regarding drought stress, ARR-B genes participate in sophisticated transcriptional networks that intersect with abscisic acid (ABA) signaling pathways. Although primarily associated with cytokinin responses, Arabidopsis ARR1, ARR10, and ARR12 form a core regulatory module that crosstalks with multiple hormone signaling cascades, modulating stomatal movement and water balance under water deficit [47–48]. The functional redundancy of ARR-Bs ensures the robustness of drought resistance signaling pathways [44]. In agreement with these conserved functions, nearly all ClARR-B members in watermelon were strongly up-regulated under drought treatment, except for the repressed *ClARR-B8*, demonstrating that the ClARR-B family is extensively involved in drought stress regulation.

In response to low-temperature stress, ARR-B genes display specific expression dynamics that contribute to plant cold acclimation. Melon CmRR6 responds actively to cold stress, implying the conserved involvement of cucurbit ARR-Bs in cold signal transduction [47]. ARR-Bs are speculated to modulate cold-responsive genes and interact with CBF signaling modules, representing a conserved adaptive pathway across plant species [30]. In this study, watermelon *ClARR-B1/2/3/4* were significantly induced by cold stress, whereas *ClARR-B5/6* were down-regulated, and other members showed no obvious changes. These distinct responses further illustrate the subfunctionalization of duplicated ClARR-B genes in cold stress regulation.

Beyond stress responsiveness, plant ARR-B genes are widely involved in tissue development and growth regulation with diversified spatial expression patterns. In watermelon, ClARR-B members exhibited tissue-specific expression in roots, stems, leaves, flowers, and fruits. Among them, *ClARR-B1* and *ClARR-B2* were constitutively and highly expressed in all tested tissues, while several other members showed extremely low transcript abundance, indicating that duplicated ClARR-B paralogs have undergone expression differentiation to coordinate watermelon growth and development. Collectively, the multi-stress response diversity and tissue-specific expression of watermelon ClARR-B genes confirm that gene duplication and subsequent subfunctionalization endow the ARR-B family with dual roles in regulating plant development and multi-abiotic stress tolerance, providing valuable candidate genes for improving crop stress resistance.

Conclusion

This study identified 10 ClARR-B genes unevenly distributed across five chromosomes in the watermelon genome. Phylogenetic analysis classified these genes into three major clades with two subgroups in Class Ⅱ, and members within the same clade exhibited highly conserved gene structures, protein motifs, and functional domains. Promoter cis-element analysis revealed that ClARR-B genes contain abundant hormone- and stress-related regulatory elements, suggesting their potential roles in hormone signal transduction and abiotic stress responses. Tissue expression analysis demonstrated that ClARR-B genes display distinct tissue-specific expression patterns, among which *ClARR-B1* and *ClARR-B2* were

constitutively highly expressed in all tested tissues. Furthermore, most ClARR-B members responded differentially to drought, salt, and cold stresses. Notably, *ClARR-B1*, *ClARR-B2*, and *ClARR-B3* were consistently up-regulated under all three abiotic stress conditions, indicating that they serve as core candidate genes for watermelon multi-stress tolerance. These results provide a comprehensive understanding of the evolutionary characteristics and functional diversity of the watermelon ARR-B family and offer valuable genetic resources for the molecular improvement of stress-resistant watermelon varieties.

Materials and methods

Identification and physicochemical property prediction of ClARR-B genes

The reference genome, protein sequences and annotation files of watermelon (*Citrullus lanatus subsp. vulgaris* cv. 97103, version V2) were retrieved from the Cucurbit Genomics Database (http://cucurbitgenomics.org/organism/21) [48]. Genomic resources including reference genome, protein sequences, annotation information and documented ARR-B family members of *Arabidopsis thaliana* L. were downloaded from the TAIR database (https://www.arabidopsis.org/index.jsp). Hidden Markov model (HMM) profile corresponding to the conserved domain of ARR-B family was obtained from the Pfam database (http://pfam.xfam.org/) [49].

To reliably identify ClARR-B candidates, HMM search against the watermelon protein dataset was performed via the hmmer software using the downloaded ARR-B HMM profile [50]. Meanwhile, a BLAST search was implemented against watermelon proteome with wheat ARR-B protein sequences as query sequences. All candidate sequences retrieved from the above two strategies were subjected to conserved domain verification via the NCBI Conserved Domain Database (CDD, http://www.ncbi.nlm.nih.gov/Structure/cdd/wrpsb.cgi), and sequences harboring complete ARR-B conserved domain were retained as final candidates [51]. The TBtools software was adopted to calculate fundamental physicochemical parameters, including amino acid length, molecular weight and isoelectric point of all identified ClARR-B proteins [52]. Subcellular localization of each ClARR-B member was further predicted using the online tool Cell-PLoc 2.0 (http://www.csbio.sjtu.edu.cn/bioinf/Cell-PLoc-2/) [53].

Chromosomal localization and gene structure analysis of ClARR-B genes

Chromosome length information and physical positions of identified ClARR-B genes were downloaded from the Cucurbit Genomics Database (http://cucurbitgenomics.org/), and chromosomal distribution map of ClARR-B members was visualized using TBtools software. Genomic and CDS sequences of watermelon ClARR-B genes were retrieved from CuGenDB. The exon-intron architecture was characterized via GSDS 2.0 online server (http://gsds.gao-lab.org/) [54], and conserved protein motifs

were predicted using the MEME suite (http://meme-suite.org/tools/meme) [55]. TBtools was finally applied to integrate and visualize gene structure and conserved motif results simultaneously [56].

Phylogenetic relationship and promoter cis-element analysis of ClARR-Bs

Amino acid sequences of ARR-B proteins from watermelon, melon, cucumber, bottle gourd, wax gourd, *Arabidopsis thaliana* and wheat were obtained from CuGenDB (http://cucurbitgenomics.org/), TAIR (https://www.arabidopsis.org/) and Ensembl Plants (https://plants.ensembl.org/index.html). Multiple sequence alignment of all ARR-B protein sequences was conducted by MUSCLE (http://www.drive5.com/muscle/), and raw alignment outputs were manually curated with Jalview software (http://www.jalview.org/) [57]. The phylogenetic tree was constructed jointly based on MUSCLE-aligned sequences using IQ-TREE with bootstrap values set at 1000 replicates [58]. Approximately 2000 bp upstream genomic sequences from the translation start site of each ClARR-B gene were extracted from CuGenDB. Cis-acting regulatory elements within promoter regions were predicted by PlantCARE database (http://bioinformatics.psb.ugent.be/webtools/plantcare/html/) [59], and the distribution and abundance of predicted cis-elements were displayed via TBtools.

Prediction of secondary and tertiary structures of ClARR-B proteins

The secondary structural features of ClARR-B proteins were predicted using the SOPMA online tool [60]. Homology-based three-dimensional structural modeling of each ClARR-B protein was performed on the SWISS-MODEL platform (https://swissmodel.expasy.org/interactive#sequence) [61].

Tissue expression profiling of ClARR-B gene family

Different watermelon tissue samples were rapidly ground into fine powder with liquid nitrogen to avoid RNA degradation. Total RNA was isolated following the manufacturer's protocols of Huayueyang RNA extraction kit(Beijing, China) under RNase-free conditions. RNA integrity and concentration were verified by agarose gel electrophoresis and P200 + ultra-micro spectrophotometer (Plextech, USA). First-strand cDNA was synthesized via two-step reverse transcription using Vazyme reverse transcription kit(Nanjing, China). qRT-PCR primers spanning single intron for each ClARR-B gene were designed based on sequence information from CuGenDB and NCBI-BLAST database (https://blast.ncbi.nlm.nih.gov/Blast.cgi). ClActin was selected as the internal reference gene. Quantitative real-time PCR was carried out on StepOnePlus™ Real-Time PCR System (Thermo Scientific, USA) following the kit instructions, with three biological replicates and three technical replicates per sample. The relative gene expression levels were calculated by the $2^{-\triangle\triangle Ct}$ method.

Expression patterns of ClARR-B genes under drought, salt and cold stresses

The experiment was carried out in the Laboratory of Cucurbit Genomics and Molecular Breeding, College of Horticulture, Henan Agricultural University. Watermelon seedlings of cultivar G42 with uniform robust growth at the five-leaf-one-heart stage were cultivated in an artificial growth chamber under conditions of 28°C, 16 h light/8 h dark, and 70% relative humidity, then subjected to three abiotic stress treatments: drought stress (root irrigation with 500 mL 300 mmol/L mannitol solution), salt stress (root irrigation with 500 mL 250 mmol/L NaCl solution), and cold stress (artificial growth chamber at 4°C, 16 h light/8 h dark, 70% relative humidity). Seedlings were sampled after obvious phenotypic alterations (3 days for drought, salt, and cold treatments separately). Three biological replicates were set for each sample. Young leaf tissues were collected and quickly ground into fine powder in a liquid nitrogen-filled mortar; All samples were ground thoroughly in liquid nitrogen to prevent RNA degradation. Total RNA of each tissue sample was extracted following the protocols of the Huayueyang RNA Extraction Kit (Beijing), with strict RNase-free operation throughout the extraction process. RNA integrity and quality were verified via agarose gel electrophoresis and an ultra-micro spectrophotometer (P200+, Plextech, USA). First-strand cDNA was synthesized from qualified RNA using a two-step reverse transcription procedure with the Vazyme reverse transcription kit.

Declarations

Acknowledgements

Not applicable.

Authors' contributions

D.L. and L.Y. conceived and designed the research. W.Y., Y.C. and H.Z. guided the experiment. H.L. and A.H. conducted the experiments. H.L. and D.L. wrote the manuscript. J.D., H.N., Y.C. and A.H. provided technical assistance. H.L. and W.K. critically reviewed and revised the manuscript. All authors have read and agreed to the published version of the manuscript.

Funding

This work was supported by the National Natural Science Foundation of China (No. 32573024).

Ethics approval and consent to participate.

Not applicable.

Consent for publication

Not applicable.

Competing interests

The authors declare no competing interests.

Author details

College of Horticulture, Henan Agricultural University, Zhengzhou 450046, China

References

1. Smiti K, Mina U, Verma M, Arya L. Impact of climate extremes and other key abiotic stresses on cucurbits: A systematic review. Vegetos. 2025;1–21.
2. Ren K, Tang T, Kong W, Su Y, Wang Y, Cheng H, Yang Y, et al. Response of watermelon to drought stress and its drought-resistance evaluation. Plants. 2025;14(9):1289.
3. Song Y, Zhang H, Wang Z, Liu B, Wang ZN. Trihelix transcription factors: versatile regulators in plant growth and development, abiotic, and biotic stress responses. Plant Cell Rep. 2026;45(1):20.
4. Zhang S, Zhu Y, Yu H, Yao S, Xiao T, Yang Y, et al. Comprehensive genomic analysis and expression profiling of the C2H2 zinc finger protein family under abiotic stresses in cucumber (Cucumis sativus L). Genes. 2020;11(2):171.
5. Yan X, Yue Z, Pan X, Si F, Li J, Chen X, Li X, et al. The HD-ZIP gene family in watermelon: genome-wide identification and expression analysis under abiotic stresses. Genes. 2022;13(12):2242.
6. Lan GP, Xuan CQ, Guo YD, Huang X, Feng MJ, Yuan L, et al. The transcription factor ClWRKY61 interacts with ClLEA55 to enhance salt tolerance in watermelon. Hortic Res. 2025;12(3):uhae320.
7. Wang X, Guo H, Jin Z, Ding Y, Guo M. Comprehensive characterization of B-Box Zinc Finger Genes in *Citrullus lanatus* and their response to hormone and abiotic stresses. Plants. 2023;12(14):2634.
8. Makino S, Kiba T, Imamura A, et al. Genes encoding pseudo-response regulators: insight into His-to-Asp phosphorelay and circadian rhythm in *Arabidopsis thaliana*. Plant Cell Physiol. 2000;41(6):791–803.
9. Huo R, Liu Z, Yu X, Li Z. The interaction network and signaling specificity of two-component system in *Arabidopsis*. Int J Mol Sci. 2020;21(14):4898.
10. Mizuno T. Plant response regulators implicated in signal transduction and circadian rhythm. Curr Opin Plant Biol. 2004;7(5):499–505.
11. Ren B, Liang Y, Deng Y, Chen Q, Zhang J, Yang X, et al. Genome-wide comparative analysis of type-A *Arabidopsis* response regulator genes by overexpression studies reveals their diverse roles and regulatory mechanisms in cytokinin signaling. Cell Res. 2009;19(10):1178–90.
12. Navarro-Cartagena S, Micol JL. Is auxin enough? Cytokinins and margin patterning in simple leaves. Trends Plant Sci. 2023;28(1):54–73.
13. Pokimica N, Ćosić T, Uzelac B, Ninković S, Raspor M. Dissecting the roles of the cytokinin signaling network: The case of de novo shoot apical meristem formation. Biomolecules. 2024;14(3):381.
14. To JPC, Deruère J, Maxwell BB, Morris VF, Kieber JJ. Cytokinin regulates type-A *Arabidopsis* response regulator activity and protein stability via two-component phosphorelay. Plant Cell. 2007;19(12):3901–14.

15. Lu J, Chen YN, Yin TM. Expression and functional divergence of a type-A response regulator paralog pair formed by dispersed duplication during Populus deltoides evolution. Commun Biol. 2024;7(1):1367.
16. Yokoyama A, Yamashino T, Amano YI, Tajima Y, Imamura A, Sakakibara H, et al. Type-B ARR transcription factors, ARR10 and ARR12, are implicated in cytokinin-mediated regulation of protoxylem differentiation in roots of *Arabidopsis thaliana*. Plant Cell Physiol. 2007;48(1):84–96.
17. Zhou CM, Li JX, Zhang TQ, Xu ZG, Ma ML, Zhang P, et al. The structure of B-ARR reveals the molecular basis of transcriptional activation by cytokinin. Proc Natl Acad Sci USA. 2024;121(3):e2319335121.
18. Kakimoto T. Perception and signal transduction of cytokinins. Annu Rev Plant Biol. 2003;54(1):605–27.
19. Rieger J, Fitz M, Fischer SM, Wallmeroth N, Flores-Romero H, Fischer NM, et al. Exploring the Binding Affinity of the ARR2 GARP DNA Binding Domain via Comparative Methods. Genes. 2023;14(8):1638.
20. Zubo YO, Schaller GE. Role of the cytokinin-activated type-B response regulators in hormone crosstalk. Plants. 2020;9(2):166.
21. Hill K, Mathews DE, Kim HJ, Street IH, Wildes SL, Chiang YH, et al. Functional characterization of type-B response regulators in the *Arabidopsis* cytokinin response. Plant Physiol. 2013;162(1):212–24.
22. Wallmeroth N, Anastasia AK, Harter K, Berendzen KW, Mira-Rodado V. *Arabidopsis* response regulator 22 inhibits cytokinin-regulated gene transcription in vivo. Protoplasma. 2017;254(1):597–606.
23. Alshegaihi RM, Alshamrani SM. Genome-wide identification of CaARR-Bs transcription factor gene family in pepper and their expression patterns under salinity stress. PeerJ. 2023;11:e16332.
24. Chen Z, Cortes L, Gallavotti A. Genetic dissection of cis-regulatory control of ZmWUSCHEL1 expression by type B RESPONSE REGULATORS. Plant Physiol. 2024;194(4):2240–48.
25. Yang H, Zhang Q, Li Z, Zhao R, Liu X, Chi Y, et al. Molecular characterization of the cytokinin responsive type-B response regulators in perennial ryegrass highlights *LpARR10* conferring salt tolerance via trans-activating SOS1 and SOS3. Environ Exp Bot. 2024;217:105566.
26. Cao H, Ding S, Li K, Zhang L, Yi Y, Li C, et al. Genome-wide identification of the ARR-B gene family and functional characterization of *OsRR41* as a positive regulator of salinity tolerance in rice. Mol Breed. 2026;46(4):34.
27. Wang J, Xia J, Song Q, Liao X, Gao Y, Zheng F, et al. Genome-wide identification, genomic organization and expression profiles of SlARR-B gene family in tomato. J Appl Genet. 2020;61(3):391–404.
28. Zeng J, Zhu X, Haider MS, Wang X, Zhang C, Wang C. Genome-wide identification and analysis of the type-B authentic response regulator gene family in peach (Prunus persica). Cytogenet Genome Res. 2017;151(1):41–9.

29. He L, Chen R, Chen Z, Lin J, Jin X, Ren C, et al. The molecular characteristics of soybean ARR-B transcription factors. Biocell. 2022;46(6):1575–83.
30. Jiang JJ, Li N, Chen WJ, Wang Y, Rong H, Xie T, et al. Genome-wide analysis of the type-B authentic response regulator gene family in Brassica napus. Genes. 2022;13(8):1449.
31. Chen H, Xue J, Zhang Z, Zhang G, Xu X, Li H, et al. High-speed rail model reveals the gene tandem amplification mediated by short repeated sequence in eukaryote. Sci Rep. 2022;12(1):2289.
32. Wang B, Xiao Y, Yan M, Fan W, Zhu Y, Li W, et al. Gene duplication and functional diversification of MADS-box genes in Malus× domestica following WGD: implications for fruit type and floral organ evolution. Int J Mol Sci. 2024;25(16):8962.
33. Dupouy G, Cashell R, Brychkova G, Tuteja R, McKeown PC, Spillane C. PICKLE RELATED 2 is a neofunctionalized gene duplicate under positive selection with antagonistic effects to the ancestral PICKLE gene on the seed transcriptome. Genome Biol Evol. 2023;15(11):evad191.
34. Huang Y, Chen J, Dong C, Sosa D, Xia S, Ouyang Y, et al. Species-specific partial gene duplication in *Arabidopsis thaliana* evolved novel phenotypic effects on morphological traits under strong positive selection. Plant Cell. 2022;34(2):802–17.
35. Yue C, Chen Q, Hu J, Li C, Luo L, Zeng L. Genome-wide identification and characterization of GARP transcription factor gene family members reveal their diverse functions in tea plant (Camellia sinensis). Front Plant Sci. 2022;13:947072.
36. Shi Y, Ding G, Shen H, Li Z, Li H, Xiao G. Genome-wide identification and expression profiles analysis of the authentic response regulator gene family in licorice. Front Plant Sci. 2024;14:1309802.
37. Fang Y, Jiang J, Hou X, Guo J, Li X, Zhao D, et al. Plant protein-coding gene families: Their origin and evolution. Front Plant Sci. 2022;13:995746.
38. Hu X, Hao J, Pan L, Xu T, Ren L, Chen Y, et al. Genome-wide analysis of tandem duplicated genes and their expression under salt stress in seashore paspalum. Front Plant Sci. 2022;13:971999.
39. Zhu XG, Hutang GR, Gao LZ. Ancient duplication and lineage-specific transposition determine evolutionary trajectory of ERF subfamily across angiosperms. Int J Mol Sci. 2024;25(7):3941.
40. Feng S, Li N, Chen H, Liu Z, Li C, Zhou R, et al. Large-scale analysis of the ARF and Aux/IAA gene families in 406 horticultural and other plants. Mol Hortic. 2024;4(1):13.
41. Ma L, Zhang T, Ye S, Lin W, Lv Y, Liu W et al. Subfunctionalization, neofunctionalization, and nonfunctionalization of the four soybean phytochrome A genes. Plant Sci. 2025;112691.
42. Cui L, Cheng H, Yang Z, Xia C, Zhang L, Kong X. Comparative analysis reveals different evolutionary fates and biological functions in wheat duplicated genes (Triticum aestivum L). Plants. 2023;12(17):3021.
43. Bruno L, Ronchini M, Binelli G, Muto A, Chiappetta A, Bitonti MB, et al. A study of GUS expression in *Arabidopsis* as a tool for the evaluation of gene evolution, function and the role of expression derived from gene duplication. Plants. 2023;12(10):2051.

44. Xie M, Chen H, Huang L, O'Neil RC, Shokhirev MN, Ecker JR. A B-ARR-mediated cytokinin transcriptional network directs hormone cross-regulation and shoot development. Nat Commun. 2018;9(1):1604.
45. Waadt R, Seller CA, Hsu PK, Takahashi Y, Munemasa S, Schroeder JI. Plant hormone regulation of abiotic stress responses. Nat Rev Mol Cell Biol. 2022;23(10):680–94.
46. Yang H, Zhang Q, Li Z, Zhao R, Liu X, Chi Y, et al. Molecular characterization of the cytokinin responsive type-B response regulators in perennial ryegrass highlights LpARR10 conferring salt tolerance via trans-activating SOS1 and SOS3. Environ Exp Bot. 2024;217:105566.
47. Li L, Zhang X, Ding F, Hou J, Wang J, Luo R, et al. Genome-wide identification of the melon (Cucumis melo L.) response regulator gene family and functional analysis of CmRR6 and CmPRR3 in response to cold stress. J Plant Physiol. 2024;292:154160.
48. Guo S, Zhang J, Sun H, Salse J, Lucas WJ, Zhang H, et al. The draft genome of watermelon (*Citrullus lanatus*) and resequencing of 20 diverse accessions. Nat Genet. 2013;45(1):51–8.
49. Mistry J, Chuguransky S, Williams L, Qureshi M, Salazar GA, Sonnhammer EL, et al. Pfam: The protein families database in 2021. Nucleic Acids Res. 2021;49(D1):D412–9.
50. Finn RD, Clements J, Eddy SR. HMMER web server: interactive sequence similarity searching. Nucleic Acids Res. 2011;39(suppl2):W29–37.
51. Marchler-Bauer A, Lu S, Anderson JB, Chitsaz F, Derbyshire MK, DeWeese-Scott C, et al. CDD: a Conserved Domain Database for the functional annotation of proteins. Nucleic Acids Res. 2010;39(suppl1):D225–9.
52. Gasteiger E, ExPASy. The proteomics server for in-depth protein knowledge and analysis. Nucleic Acids Res. 2003;31(13):3784–8.
53. Chou KC, Shen HB. Cell-PLoc: A package of web-servers for predicting subcellular localization of proteins in various organisms. Nat Protoc. 2008;3(2):153–62.
54. Hu B, Jin J, Guo AY, Zhang H, Luo J, Gao G. GSDS 2.0: an upgraded gene feature visualization server. Bioinformatics. 2015;31(8):1296–7.
55. Bailey TL, Johnson J, Grant CE, Noble WS. The MEME suite. Nucleic Acids Res. 2015;43(W1):W39–49.
56. Chen C, Wu Y, Li J, Wang X, Zeng Z, Xu J, et al. TBtools-II: A one for all, all for one bioinformatics platform for biological big-data mining. Mol Plant. 2023;16(11):1733–42.
57. Edgar RC. Multiple sequence alignment with high accuracy and high throughput. Nucleic Acids Res. 2004;32(5):1792–7.
58. Minh BQ, Schmidt HA, Chernomor O, Schrempf D, Woodhams MD, Von Haeseler A, et al. IQ-TREE 2: new models and efficient methods for phylogenetic inference in the genomic era. Mol Biol Evol. 2020;37(5):1530–4.
59. Lescot M, Déhais P, Thijs G, Marchal K, Moreau Y, Van de Peer Y, et al. PlantCARE, a database of plant cis-acting regulatory elements and a portal to tools for in silico analysis of promoter

sequences. Nucleic Acids Res. 2002;30(1):325–7.

60. Geourjon C, Deleage G. SOPMA: significant improvements in protein secondary structure prediction by consensus prediction from multiple alignments. Bioinformatics. 1995;11(6):681–4.
61. Waterhouse A, Bertoni M, Bienert S, Studer G, Tauriello G, Gumienny R, et al. SWISS-MODEL: homology modelling of protein structures and complexes. Nucleic Acids Res. 2018;46(W1):W296–303.

Figures

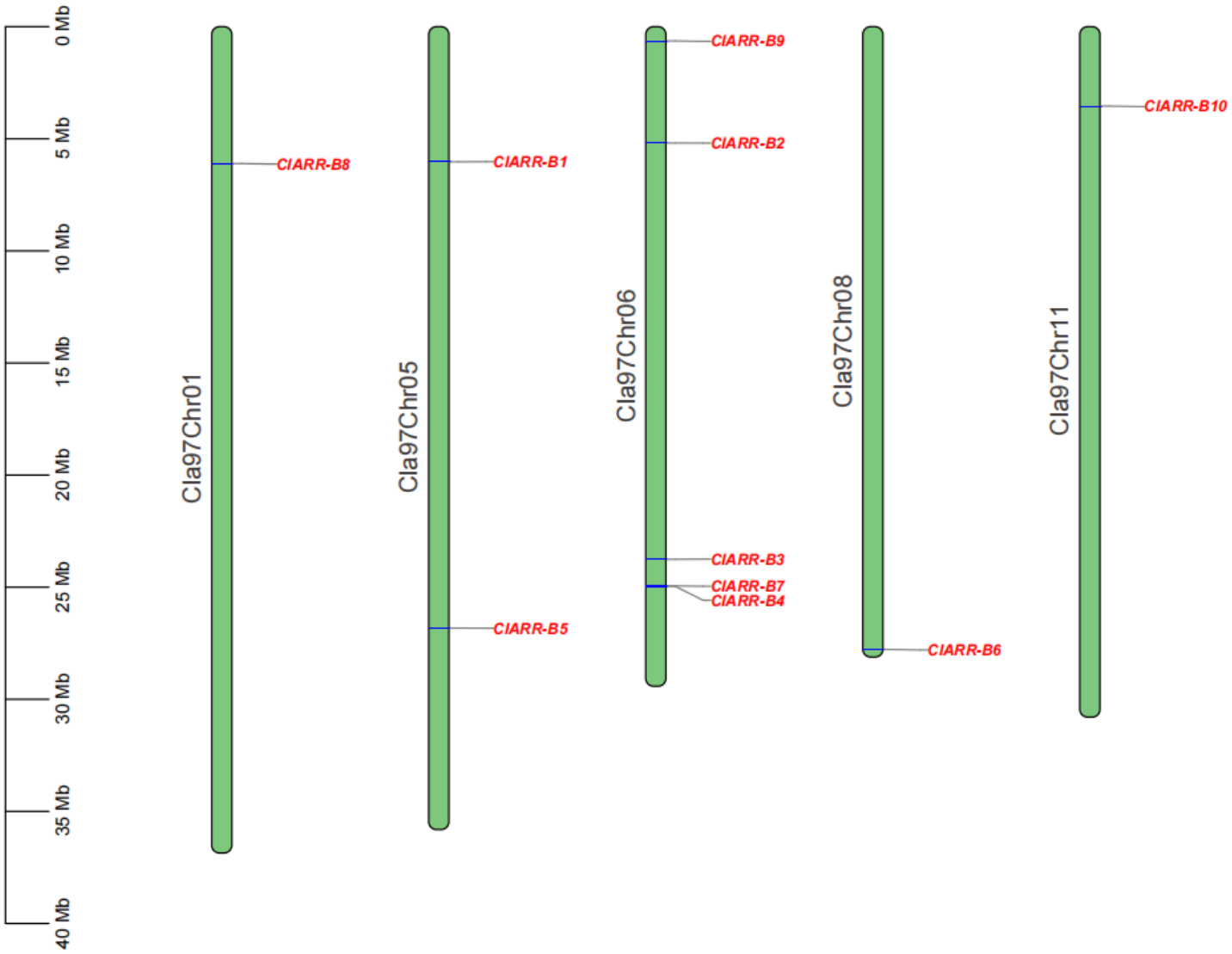

Figure 1

Chromosomal positions of the ClARR-B gene family members

Green bars represent the five chromosomes with ClARR-B genes. The scale indicates the chromosome length, and the blue lines indicate the position of each ClARR-B gene.

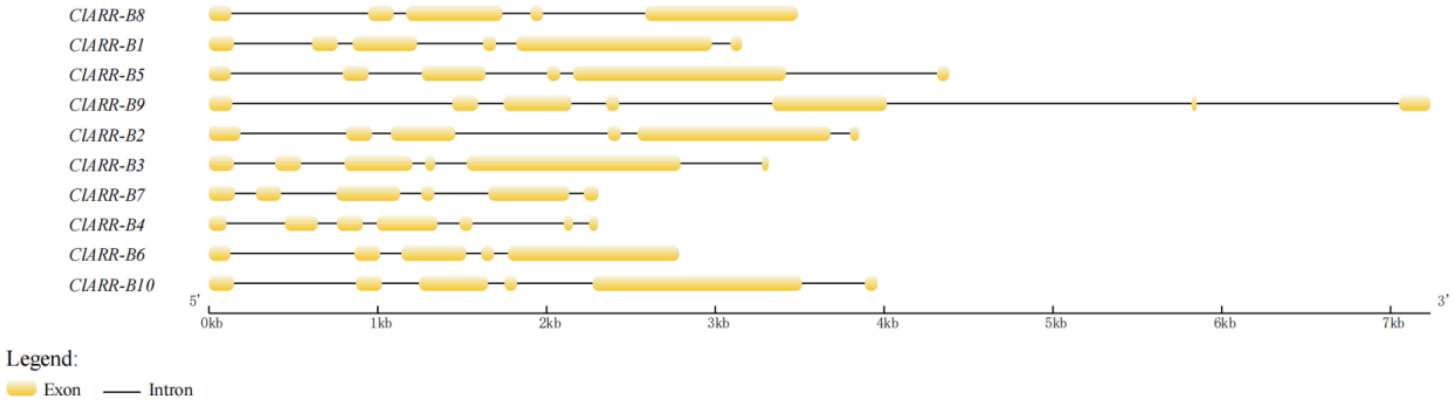

Figure 2

Gene structures of the ClARR-B family members

Exon-intron structure of ClARR-B genes. Yellow boxes and black lines represent exons and introns. The scale indicates the gene length

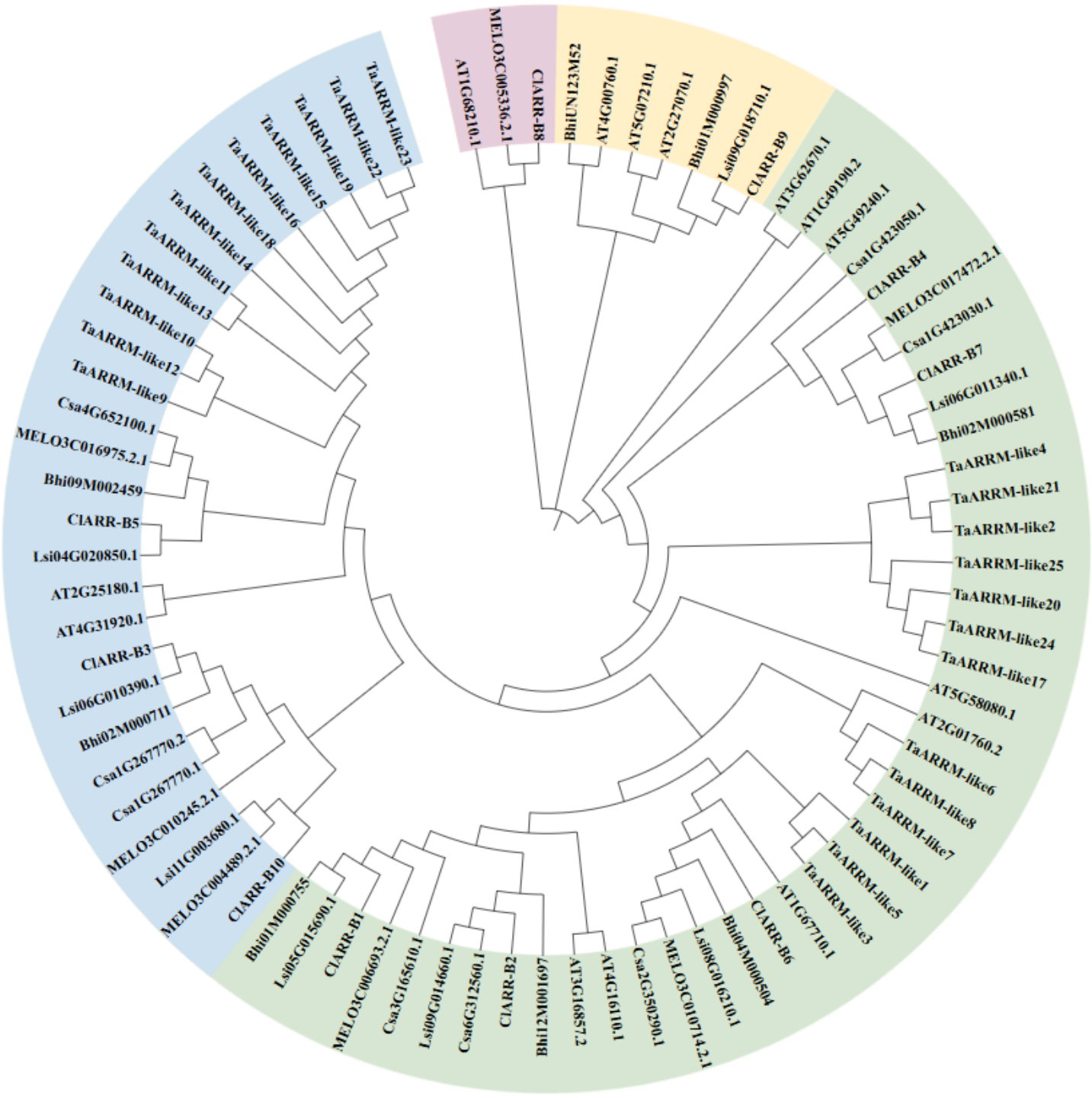

Figure 3

Phylogenetic analysis of the ARR-B genes family members in watermelon, muskmelon, cucumber, wax gourd, bottle gourd, Arabidopsis thaliana and wheat

The phylogenetic tree is divided into four groups (Class Ⅰ, Class Ⅱ, Class ⅡA and Class ⅡB)

The background is shaded in purple, yellow, green,and blue for Class Ⅰ, Class Ⅱ, Class ⅡA and Class ⅡB, respectively

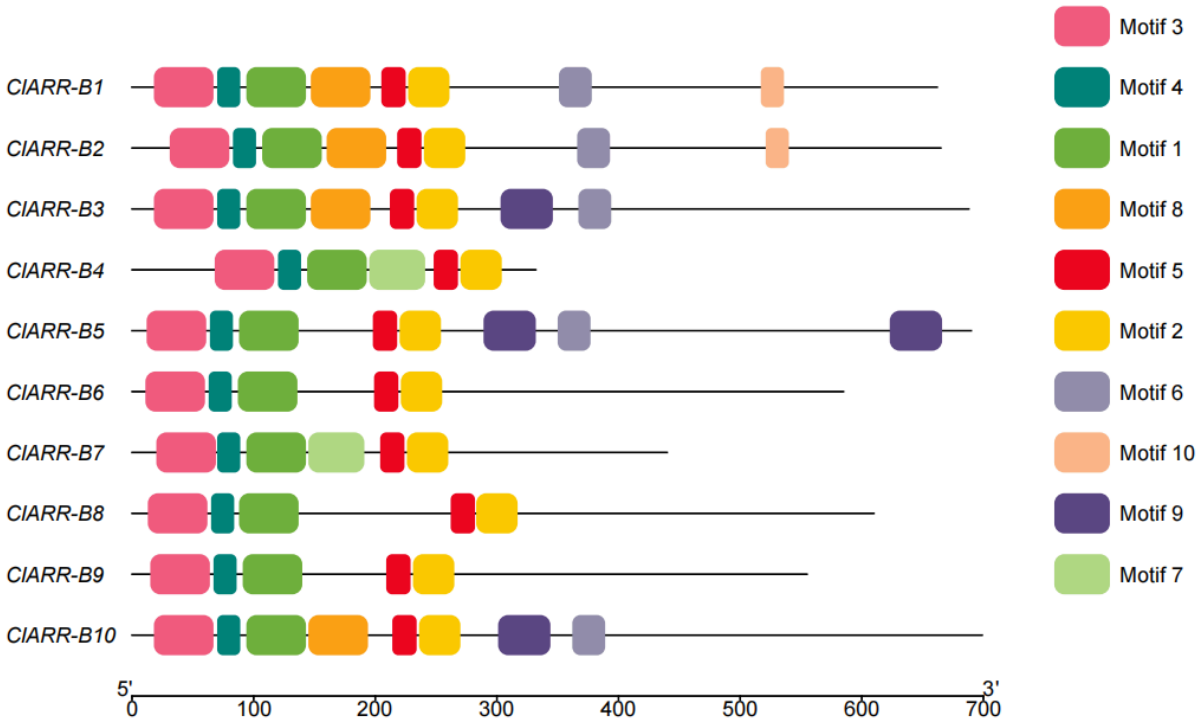

Figure 4

Conserved motif analysis of the ClARR-B gene family members

Distribution of conserved motifs in ClARR-B proteins. Different motifs are represented by numbered colored boxes. The scale indicates the gene length

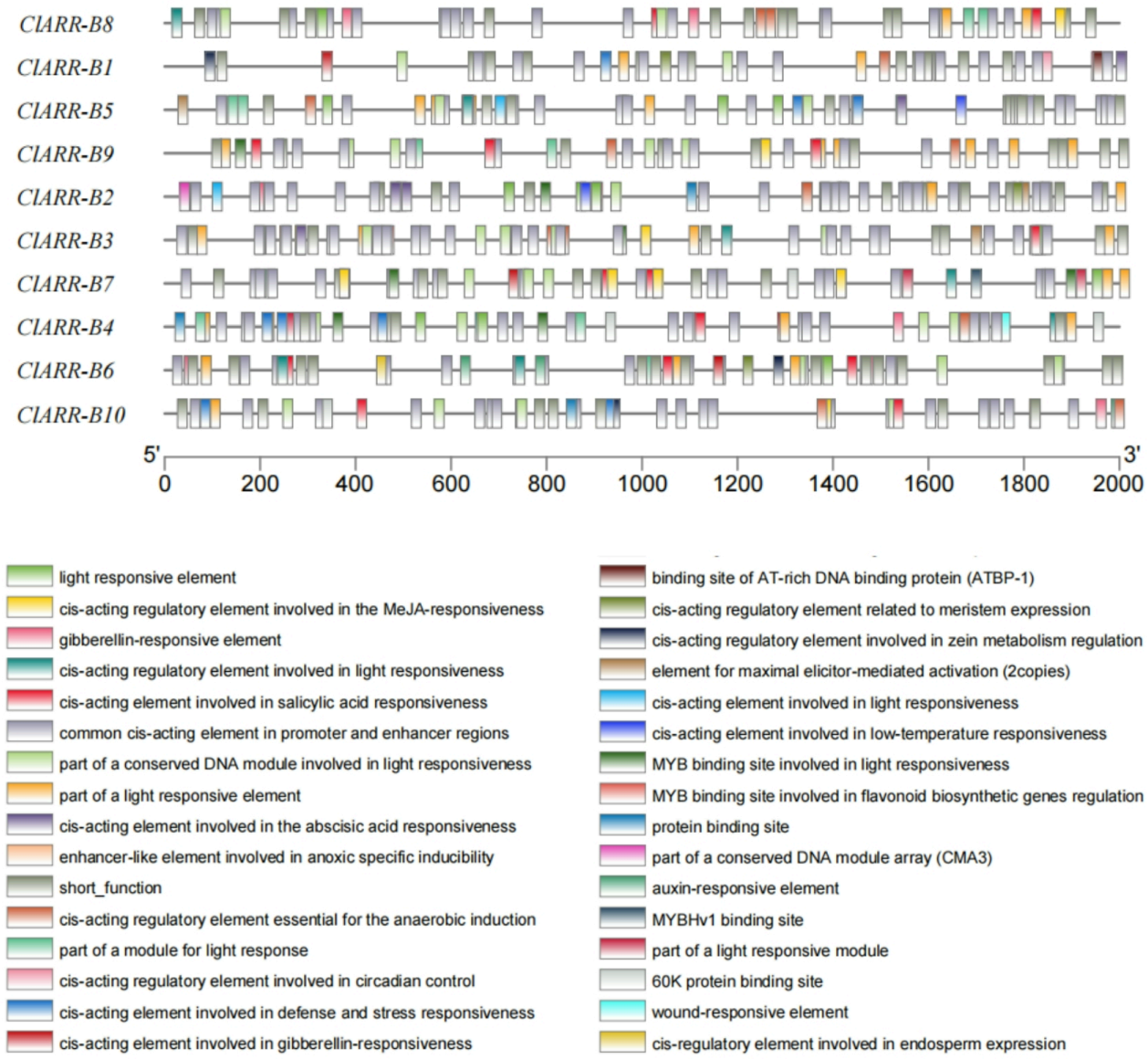

Figure 5

Cis-acting element analysis of the promoters of ClARR-B gene family members

Distribution of conserved promoter cis-elements in ClARR-B promoters. Different motifs are represented by numbered colored boxes. The scale indicates the promoter length

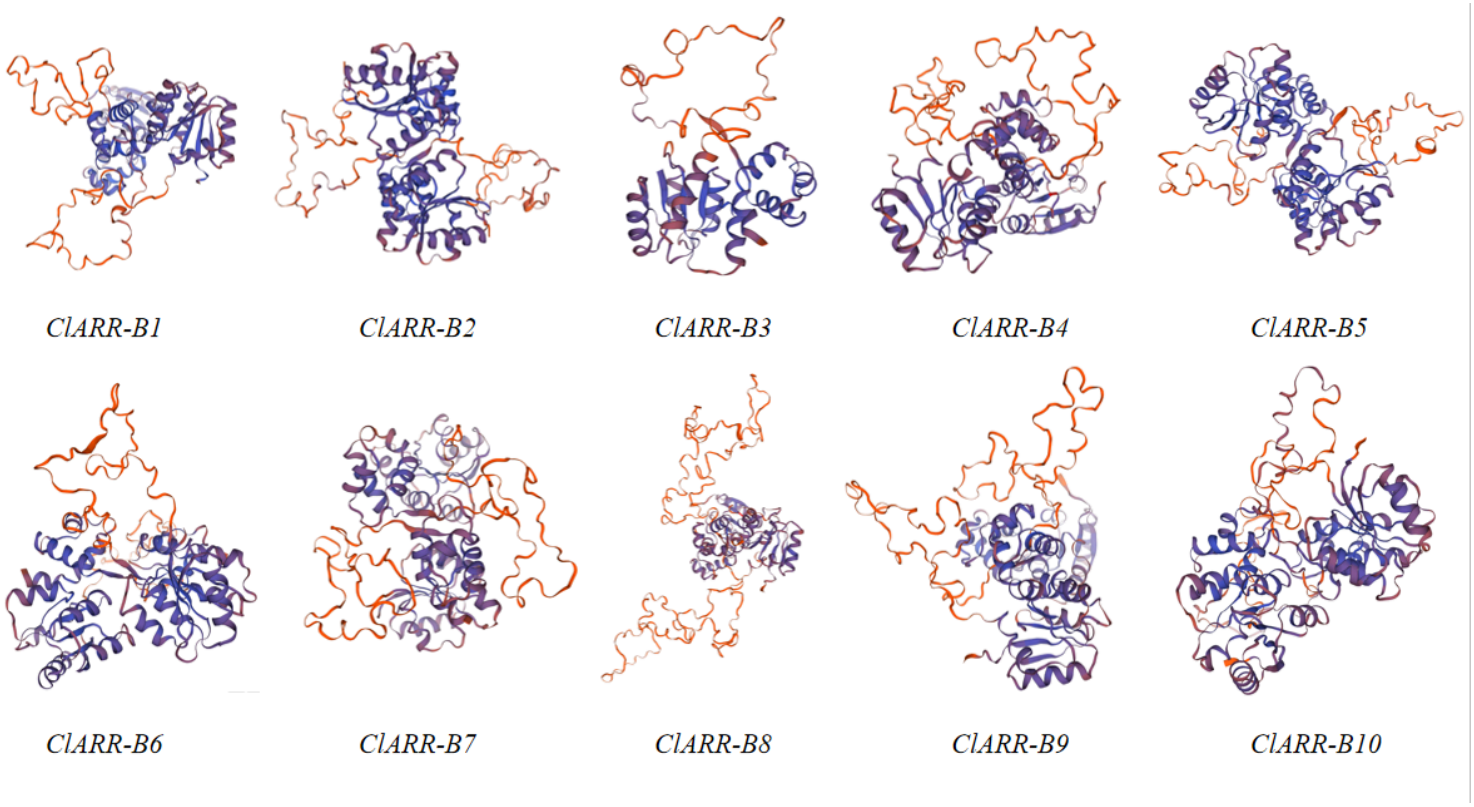

Figure 6

Predicted 3D structural models of the proteins encoded by ClARR-B gene family members

Significant structural differences were observed among ClARR-B proteins from distinct phylogenetic subgroups

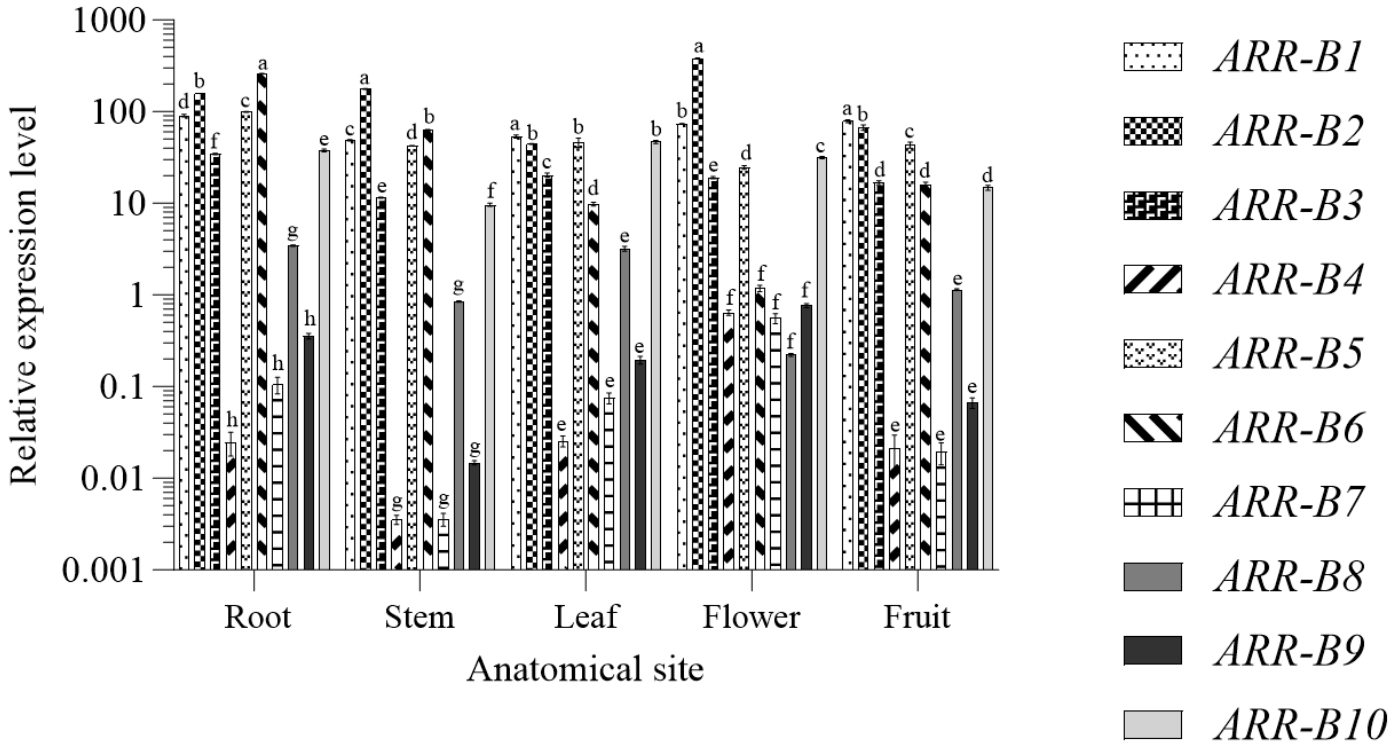

Figure 7

Relative expression levels of the ClARR-B gene family members in different tissues

Expression levels of 10 ClARR-B genes in different tissues of watermelon cultivar G42. Relative expression levels were quantified by qRT-PCR with ClActin as the internal reference, and calculated using the $2^{-\triangle\triangle Ct}$ method. Lowercase letters denote statistically significant differences ($P < 0.05$) among different genes within the same tissue, as determined by one way ANOVA followed by Tukey's test. Data are shown as mean ± SD (n = 3, biological replicates).

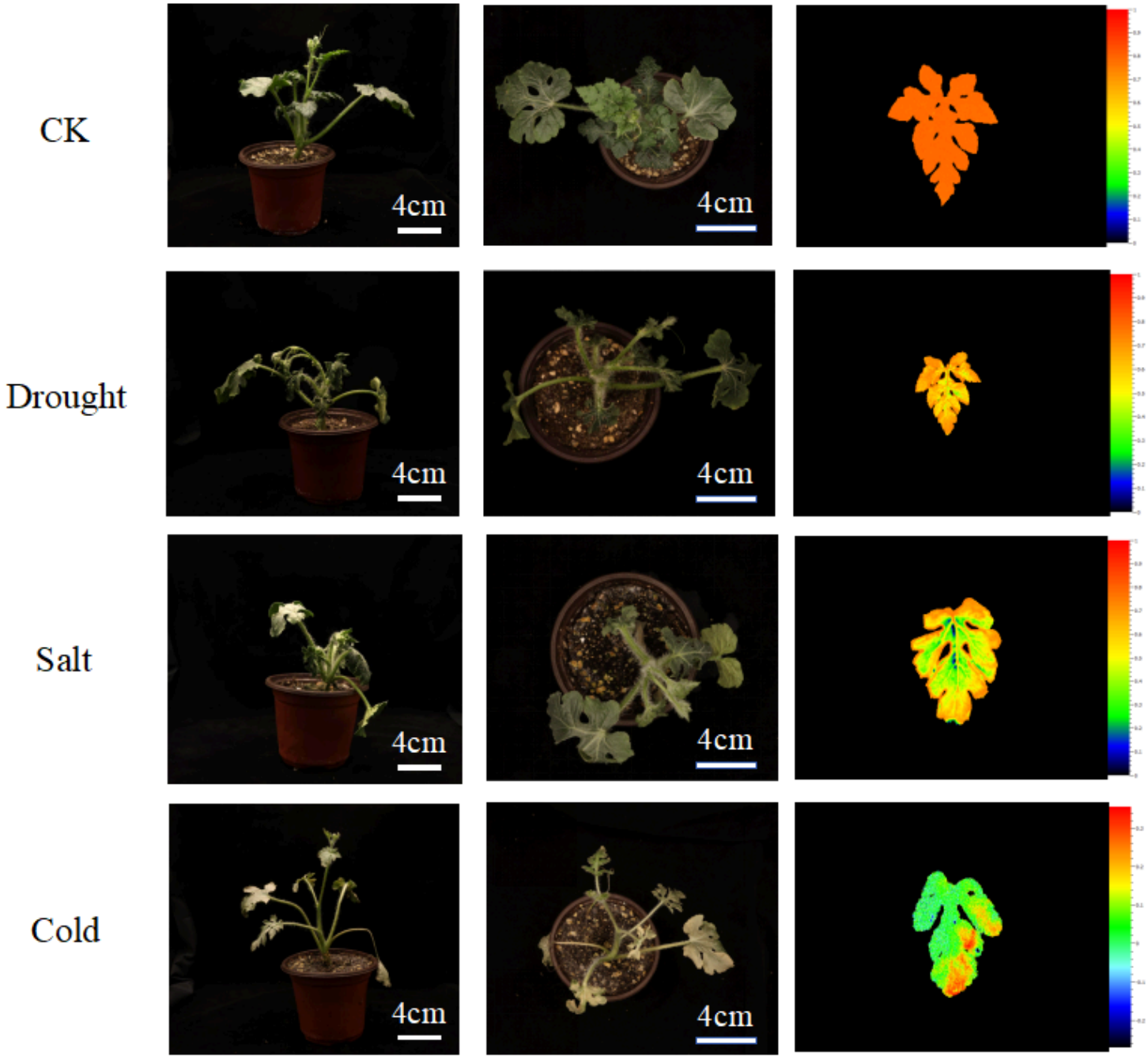

Figure 8

Seedling phenotypes and chlorophyll fluorescence parameter Fv/Fm of watermelon under drought, salt and cold stresses

All three abiotic stresses markedly decreased the Fv/Fm values of watermelon leaves, indicating that the photosynthetic function of seedlings was severely impaired

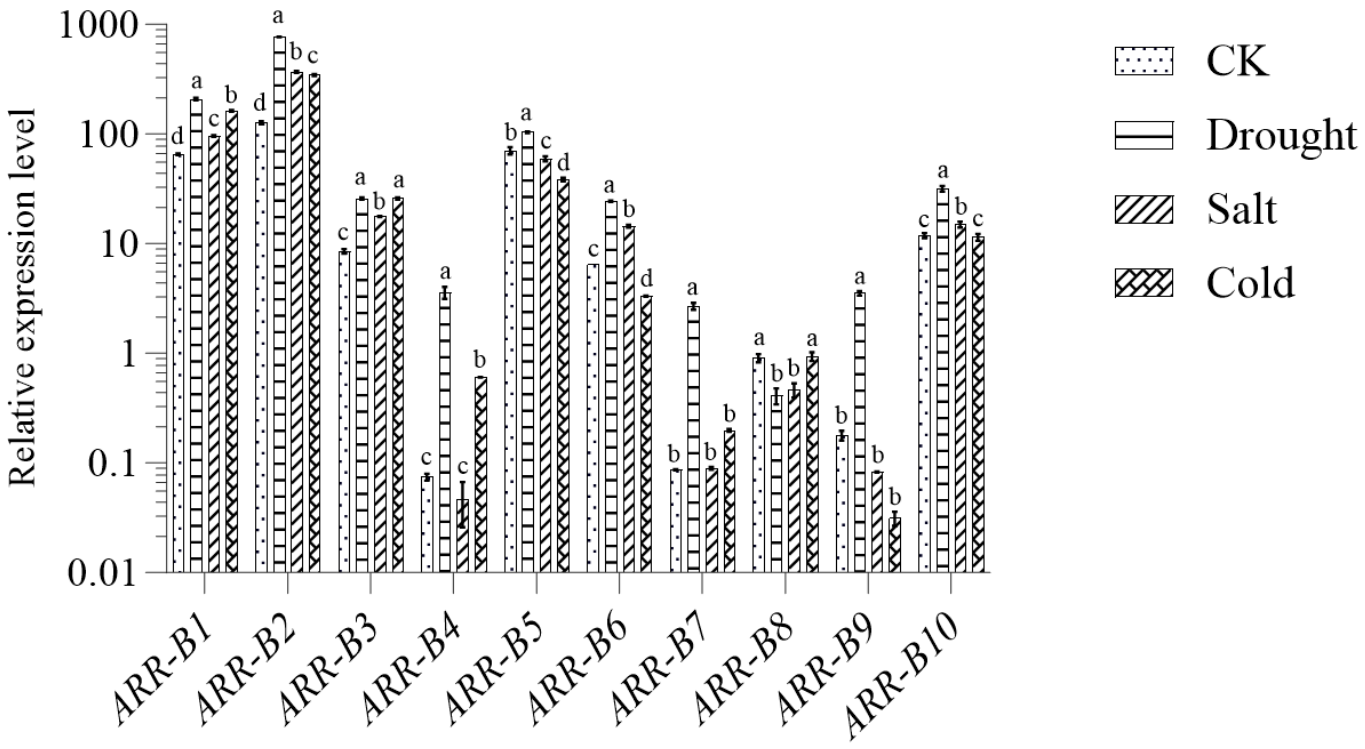

Figure 9

Relative expression levels of the ClARR-B gene family members in different abiotic stresses

Expression patterns of 10 ClARR-B genes under drought, salt and cold stresses in watermelon. Relative expression levels were determined by qRT-PCR using ClActin as an internal reference and calculated via the $2^{-\triangle\triangle Ct}$ method. Lowercase letters indicate statistically significant differences ($P < 0.05$) for the same gene among different abiotic stresses, as determined by one way ANOVA followed by Tukey's test. Data are presented as mean ± SD (n = 3, biological replicates)